Effect of wheelchair configurations on shoulder movements, push rim kinetics and upper limb kinematics while negotiating a speed bump

Gawande, Mohan; Wang, Peng; Arnold, Graham; Nasir, Sadiq; Abboud, Rami; Wang, Weijie

Published in:
Ergonomics

DOI:
10.1080/00140139.2021.2008018

Publication date:
2021

Ergonomics

ISSN: (Print) (Online) Journal homepage: https://www.tandfonline.com/loi/terg20

Effect of wheelchair configurations on shoulder movements, push rim kinetics and upper limb kinematics while negotiating a speed bump

Mohan Gawande, Peng Wang, Graham Arnold, Sadiq Nasir, Rami Abboud & Weijie Wang

To cite this article: Mohan Gawande, Peng Wang, Graham Arnold, Sadiq Nasir, Rami Abboud & Weijie Wang (2021): Effect of wheelchair configurations on shoulder movements, push rim kinetics and upper limb kinematics while negotiating a speed bump, Ergonomics, DOI: 10.1080/00140139.2021.2008018

To link to this article: https://doi.org/10.1080/00140139.2021.2008018

Published online: 29 Nov 2021.

ERGONOMICS
https://doi.org/10.1080/00140139.2021.2008018

Taylor & Francis
Taylor & Francis Group

ARTICLE

OPEN ACCESS Check for updates

Effect of wheelchair configurations on shoulder movements, push rim kinetics and upper limb kinematics while negotiating a speed bump

Mohan Gawande[a], Peng Wang[b], Graham Arnold[a], Sadiq Nasir[a], Rami Abboud[c] and Weijie Wang[a]

[a]University Department of Orthopaedic and Trauma Surgery, Tayside Orthopaedic and Rehabilitation Technology Centre, Ninewells Hospital and Medical School, Dundee University, Dundee, UK; [b]Department of New Energy, Tianjin Sino-German University of Applied Sciences, Tianjin, China; [c]Faculty of Engineering, University of Balamand, Koura, Lebanon

ABSTRACT

This study aimed to provide a comprehensive assessment of upper limb kinetics and kinematics and shoulder movements during wheelchair propulsion while negotiating a speed bump of 6 cm height using four different wheelchair configurations. 16 healthy males aged 30.8 ± 5.7 years participated in the experiment. The kinetic and kinematic data during wheelchair propulsion were recorded. A smart system was used to collect the push forces and a motion capture system was used to collect upper limb movements. The results show that approximately 50% more pushing force was required to negotiate the speed bump than that of level ground propulsion. At the upward-forward axle position, peak total forces were 95.17 ± 5.70 N which resulted in significantly improved propulsion ergonomics, but 129.36 ± 6.68 N was required at the upward-back axle position at the speed bump push. The findings could help manufactures to design protective gloves for wheelchair users and provide useful rehabilitation information to clinicians and patients.

Practitioner summary: This study investigated pushing forces and movements during wheelchair propulsion over a speed bump. Approximately 50% more pushing force was required to negotiate the bump than a level surface propulsion. The upper-forward axle position was found to be reasonably better than other positions during wheelchair propulsion.

Abbreviations: UF: upper and forward position; UB: upper and back position; DF: down and forward position; DB: down and back position; ROM: range of motion

ARTICLE HISTORY
Received 15 June 2020
Accepted 12 November 2021

KEYWORDS
Wheelchair; speed bump; push force; chair position; upper limb

1. Introduction

Manual wheelchair propulsion is a distinctive way of utilising the muscles of the upper extremities to provide mobility (Briley et al. 2020; MacGillivray et al. 2020). Nevertheless, it imposes a considerable demand upon the upper limb joints and muscles. A harmful combination of straining with overuse and repetitive actions of the upper limbs leads to the emergence of upper limb pathologies (Robertson et al. 1996). Therefore, it is paramount to minimise mechanical loads during manual propulsion and the optimisation of propulsion efficiency must be undertaken by researchers, manufacturers and clinicians to improve overall mobility for users. In manual wheelchair propulsion, obstacle negotiation is one of the most important skills to users as it requires higher energy and greater joint forces depending on the complexity of the obstacle. A considerable amount of literature has been published on the effect of axle position on wheelchair propulsion (van der Woude et al. 1989; Boninger et al. 2000; Medola et al. 2014; Wieczorek and Kukla 2019), muscle activity during propulsion (Louis and Gorce 2010; Qi et al. 2012; Weston, Khan, and Marras 2017; Hassanain et al. 2018; Stone et al. 2019), and kinetics and kinematics (Richter 2001; Cowan et al. 2009; Kotajarvi et al. 2004; Freixes et al. 2010; Dubowsky, Sisto, and Langrana 2009; Silva, Paschoarelli, and Medola 2019). The Paralysed Veterans of America Clinical Practice Guidelines on Upper Limb Preservation in Spinal Cord Injury (Paralyzed Veterans of America 2005) have evidence-based recommendations on how to properly configure a wheelchair (regarding rear axle placement), however, there is a lack of biomechanical assessment and

CONTACT Weijie Wang w.wang@dundee.ac.uk University Department of Orthopaedic and Trauma Surgery, Tayside Orthopaedic and Rehabilitation Technology Centre, Ninewells Hospital and Medical School, Dundee University, Dundee DD1 4HN, UK

evidence. Few studies have investigated obstacle negotiation (Desroches et al. 2009; Nagy et al. 2012).

To the best of our knowledge, research to date has not yet examined the relationship between wheelchair configurations, kinematics, and push rim kinetics while negotiating a speed bump. So far, there has been little research on how much pushing force is required when propelling a wheelchair over a speed bump compared to the level ground. Which configuration and axle position is better suitable for the situation? This research question was to be addressed. This research aimed to investigate whether wheelchair configuration affects push rim kinetics and kinematics of the shoulder and elbow joints in able-bodied individuals during wheelchair propulsion while negotiating a standard speed bump of 6 cm height.

2. Methods and materials

The project was carried out at the Sports Biomechanics Laboratory with a level vinyl floor at the University Department of Orthopaedic & Trauma Surgery, University of Dundee, UK. Ethical approval was obtained for this project from the University (SMED REC 081/18). Human experimentation was approved by the local institutional review board and conforms to the Helsinki Declaration. Each participant signed a consent form before data collection commenced.

2.1. Study population

Inclusion criteria: healthy non-wheelchair user with no registered shoulder or elbow injuries, disabilities and surgeries. Male participants aged between 18 and 40 years. Participants were recruited with the help of recruitment posters. Using novice participants ensured the techniques employed would not be biased by a configuration that the wheelchair user was accustomed to.

2.2. Data Collection apparatus

2.2.1. Smartwheel®

A Smartwheel® (Three Rivers Holdings, LLC, Mesa, Arizona, USA) is a modified magnesium alloy wheel used to measure three-dimensional push rim forces for each push and other mechanical parameters. The Smartwheel® was attached to the axle of the wheelchair on the dominant side of each participant. A sampling frequency of 240 Hz was used. The radius of the Smartwheel® push rim was 0.2667 m (Three Rivers Holdings 2008). Peak Total Force and its tangential component, Average Push Force (F_{tot}) and its tangential (F_t) component, Peak and Average Moment (M_z) about the wheelchair hub, Average Speed, Push angle (average range of the push in degrees during the push phase), Push Frequency (average number of pushes on the Smartwheel® per second) and Mechanical Efficiency (F_t^2/F_{tot}^2) were measured during propulsion.

2.2.2. Vicon® motion capture system

A Vicon® MX motion capture system (Vicon® Oxford Metrics, Kidlington, UK) was used for kinematic data collection. The motion capturing space was captured using 16 high-resolution cameras (1.3 and 4 megapixels in the MX system with a sampling frequency of 200 Hz). A set of 10 retro-reflective markers were attached using double-sided medical adhesive tape to the skin overlying specifically identified bony landmarks at the suprasternal notch (IJ), xiphoid process (PX), spinal processes of C7 and T8 vertebrae, the most lateral part of the acromion process (AA), at the humeral shaft along the acromion and lateral epicondyle, humeral medial (EM) and lateral (EL) epicondyles, radial (RS) and ulnar (US) styloids of the dominant side of each participant. These bony landmarks were advocated by the International Society of Biomechanics (ISB) (Wu et al. 2005) to establish body segments. The models have been validated and used in previous research studies conducted at our institute (Kolwadkar et al. 2011; Sherif et al. 2016; Kabra et al. 2015). A standard heavy-duty speed bump (made of high-density recycled rubber, the Ramp People, UK) with a width of 45 cm and a height of 6 cm was placed in the centre of the capture volume.

2.2.3. Wheelchair

The Quickie GPV range rigid frame model manufactured by Sunrise® Medical Limited, West Midlands, England, was used in this study. It is a lightweight manually propelled wheelchair weighing 11 kg. The diameter of the rear wheels is 60 cm and the diameter of the hand rim is 53.2 cm. A backrest angle was fixed at 15°. The rear wheel chamber was kept constant at 0° (Sunrise® Medical Limited, owner's manual). The sitting height of each participant was standardised by placing cushions of different heights on the seat of the wheelchair, that is, the distance between shoulder acromion and centre of the axle captured in the horizontal or vertical directions in a static pose being the same. A special (aluminium) axle plate was fabricated in order to easily change different positions of the axle, by making an 'I' shaped slot in the axle plate (Figure 1). The four different rear

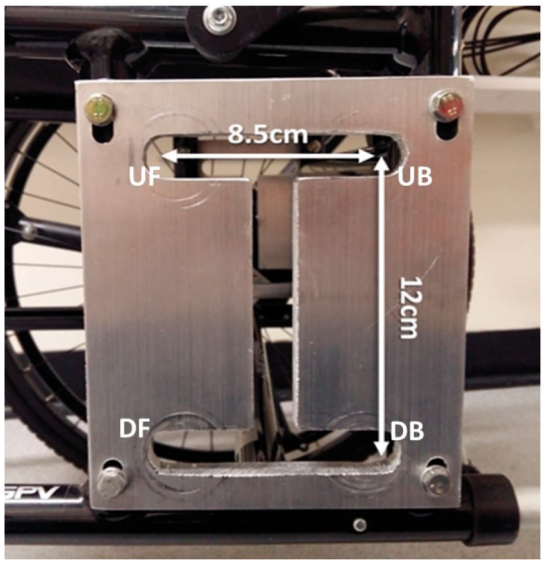

Figure 1. 'I' shaped slot in axle plate. *Note*. Four positions are upper forward (UF), upper back (UB), down forward (DF) and down back (DB).

wheel axle positions used were Upward-Forward (UF), Upward-Backward (UB), Downward-Forward (DF) and Downward-Backward (DB). These positions were considered as extreme positions and thus assumedly may give implication on which one is optimum. These axle positions were randomised during data collection and the data for five trials of each position were collected. There was a difference of 8.5 cm between the forward and backward axle positions while there was a difference of 12 cm between the upward and downward positions.

Castor wheel adjustment was done for different axle positions to maintain the same seat angle to the floor. Anti-Tip Tubes were used on the wheelchair as a safety measure.

2.3. Preparation of participant

The 10 retro-reflective markers were placed at the previously mentioned sites on the body of the participant (Figure 2). Participants were given a practice session of approximately 10 min to familiarise themselves with using the wheelchair.

2.4. Data collection

Anthropometric measurements of Height, Weight, Gender, Age were collected, and Body Mass Index was calculated. Participants were requested to propel the wheelchair forward along a 30 m long lab space at a comfortable speed and to negotiate a speed bump in the middle of the distance for all the trials (Figure 3). Each participant did approximately 10 trials, and finally, three good trials were used for further analysis. After completion of all the trials, each participant was asked about their opinion of the most comfortable axle position out of the four settings.

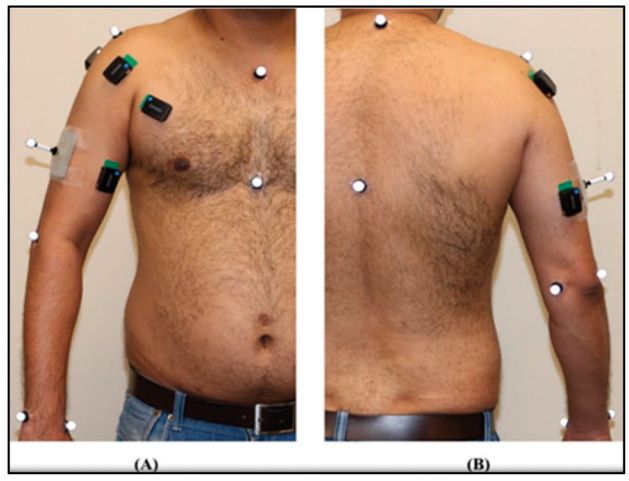

Figure 2. Retro-reflective markers used for the motion capture system. (A) Anterior view, (B) Posterior view.

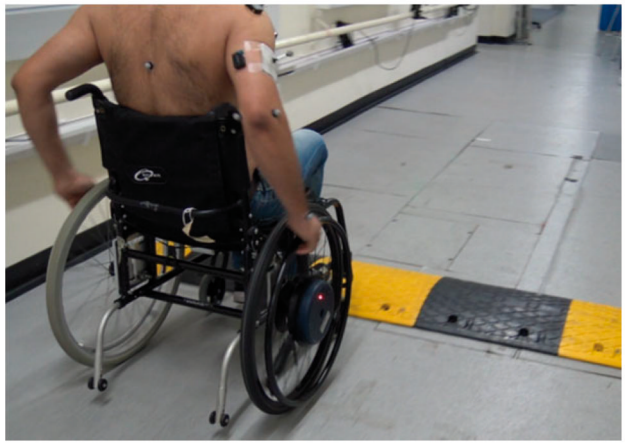

Figure 3. Negotiating the speed bump in the lab.

2.5. Data extraction and determination of cycles and phases

The labelling of the markers and determination of a cycle was completed in Nexus 2.8.1 version from Vicon® using a custom model written in BodyBuilder® locally. Each trial of wheelchair propulsion consisted of a push phase and a recovery phase. The initiation of the push phase began with initial hand contact to the push rim and the end of the push phase was decided when the hand left the push rim (Figure 4 at point 1 and point 2, respectively). The recovery phase began at the end of the push phase. The end of the recovery phase was marked by hand contact to its initial

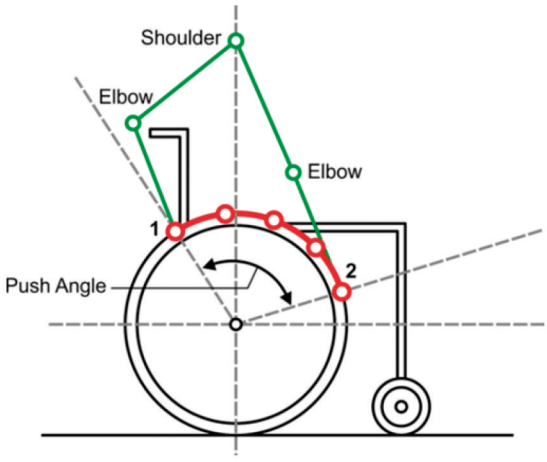

Figure 4. Phases of cycle and Push angle.

position of contact to the push rim in preparation for the next push.

Three cycles were marked in Vicon® data as the events which were 'before speed bump' cycle, 'at speed bump' cycle and 'after speed bump' cycle. The Smartwheel® data were drawn out and matched with Vicon® data by observing a sudden decrease in the speed and an increase in the push force at the speed bump. Additionally, Smartwheel® data were cropped for the first three pushes. As the first pushes are usually higher than those on level ground and thus can be used as the kinetic reference to the pushes at the speed bump (Koontz et al. 2005). The trunk movement was considered in the sagittal plane only with reference to the global coordination system. The motion of the arm and forearm were considered with reference to the local coordination system. Graphs with the shoulder and elbow joint ROM in all three X (sagittal) and Y (frontal) and Z (transverse) planes were analysed using an in-house designed software program produced using MATLAB (The MathWorks, Inc, Natick, MA, USA). The ROM was considered as the difference between the maximum and minimum degree of movement in each of the three respective planes.

2.6. Statistical analysis

Data were statistically analysed using SPSS software (version 23, IBM, Inc., Chicago, IL, USA). Data were inspected for normality by The Kolmogorov–Smirnov test (K-S). Data were paired for different wheel positions for within-subject comparisons in the general linear model for repeated measures. In other words, a two-way ANOVA test within-subject factor with posthoc comparison, Least Significant Difference and controlling for Type I errors selected was run to obtain the significant difference. The upper and down positions and forward and back positions were compared separately, and four positions were compared together. If the variables were not a normal distribution, a non-parametric test was also applied to check *p*-values. The statistically significant value was set at $p < 0.05$.

3. Results

Sixteen right-hand dominant healthy males participated in this project. Mean and standard deviation of age, weight, height and body mass index were 30.81 ± 5.74 years, 81.25 ± 10.25 kg, 175.5 ± 6.6 cm and 26.45 ± 3.40 kg/m^2, respectively.

3.1. Kinetics

The peak total forces in four positions at different pushes are shown in Table 1 where *p*-values are reported for ANOVA results and pairwise comparisons from the posthoc test are reported in Tables 1 and 2. From Tables 1–3, it was found that as a whole, the peak force total was the lowest in UF among the four positions and the peak force total at speed bump push was approximately 50% higher than for other pushes. Push rim variables at four different axle positions at 'speed bump' push are shown in Tables 4–6.

As seen in Table 4, the upper and down positions did not show significant differences in all of the variables, except mechanical effectiveness. However, in Table 5, almost all kinetic variables showed significant differences, that is, that the forward position resulted in lower values than the back position. Moreover, as seen in Table 6 of the comparisons of the four positions, the upper-forward position produced the least peak total forces and averaged total forces, meaning that the upper-forward position saves energy for participants in the most efficient way. From Tables 4–6, it was found that push angle (°), average speed (m/s) and push frequency did not change with different axle positions.

In terms of pushes in various stages of wheelchair propulsion, peak total forces of the first three pushes, 'before speed bump, 'at speed bump' and 'after speed bump' were measured as shown in Figure 5. There was approximately a 50% rise in peak total force at the 'speed bump' push as compared to 'before speed bump' and 'after speed bump' pushes. Moreover, peak total force at the 'speed bump' push was 30% greater than that of the first three initial pushes as shown in Figure 5.

At the 'speed bump' push, there was a rise of approximately 60% and 80% in the peak moment for

Table 1. Within-subjects comparison for different pushes and axle positions in peak force total.

			95% Confidence interval			
Push	Mean (*n*)	Std. error	Lower bound	Upper bound	*p*-Value	With-subjects contrasts
Start push1	114.31	3.71	106.77	121.86	0.012*	Linear
Start push2	110.75	3.20	104.22	117.27	0.105	Quadratic
Start push 3	112.74	3.46	105.71	119.78	<0.0001**	Cubic
Before bump	97.67	3.57	90.40	104.94		
At bump	157.32	3.58	150.04	164.60		
After bump	99.52	2.60	94.23	104.81		
Axle position						
UF	106.54	4.57	97.23	115.85	0.820	Linear
UB	127.89	5.35	116.99	138.79	0.021**	Quadratic
DF	114.33	3.37	107.45	121.20	0.007**	Cubic
DB	112.79	5.17	102.26	123.31		

Note. In SPSS, a general linear model for repeated measures was used with two within-subject factors, one for pushes and the other for axle position, and the number of trials was 33.
*$p < 0.05$; **$p < 0.01$.

Table 2. The post-hoc pairwise comparison for different pushes in peak force total.

Pairwise comparisons						
Measure: peak force total						
					95% confidence interval for difference[a]	
(I) push	(J) push	Mean difference (I − J)	Std. error	*p*-Value[a]	Lower bound	Upper bound
1	2	3.567	3.432	0.306	−3.424	10.558
	3	1.570	3.889	0.689	−6.350	9.491
	4	16.645	3.679	<0.0001**	9.150	24.140
	5	−43.006	4.002	<0.0001**	−51.158	−34.854
	6	14.791	3.050	<0.0001**	8.579	21.004
2	1	−3.567	3.432	0.306	−10.558	3.424
	3	−1.997	2.411	0.414	−6.909	2.915
	4	13.078	3.825	0.002**	5.287	20.868
	5	−46.574	3.852	<0.0001**	−54.420	−38.727
	6	11.224	2.052	<0.0001**	7.045	15.403
3	1	−1.570	3.889	0.689	−9.491	6.350
	2	1.997	2.411	0.414	−2.915	6.909
	4	15.075	3.128	<0.0001**	8.703	21.446
	5	−44.577	3.344	<0.0001**	−51.388	−37.765
	6	13.221	2.746	<0.0001**	7.629	18.814
4	1	−16.645	3.679	<0.0001**	−24.140	−9.150
	2	−13.078	3.825	0.002**	−20.868	−5.287
	3	−15.075	3.128	<0.0001**	−21.446	−8.703
	5	−59.651	3.562	<0.0001**	−66.907	−52.396
	6	−1.853	3.486	0.599	−8.954	5.247
5	1	43.006	4.002	<0.0001**	34.854	51.158
	2	46.574	3.852	<0.0001**	38.727	54.420
	3	44.577	3.344	<0.0001**	37.765	51.388
	4	59.651	3.562	<0.0001**	52.396	66.907
	6	57.798	3.005	<0.0001**	51.676	63.919
6	1	−14.791	3.050	<0.0001**	−21.004	−8.579
	2	−11.224	2.052	<0.0001**	−15.403	−7.045
	3	−13.221	2.746	<0.0001**	−18.814	−7.629
	4	1.853	3.486	0.599	−5.247	8.954
	5	−57.798	3.005	<0.0001**	−63.919	−51.676

[a]Adjustment for multiple comparisons: Least Significant Difference (equivalent to no adjustments). Variable 1: start push 1; 2: start push 2; 3: start push 3; 4: push before bump; 5: push at bump; 6: push after bump.
*$p < 0.05$l; **$p < 0.01$.

the DB axle position and for the other three positions respectively as compared to that of the 'before bump' push (Figure 6).

3.2. Kinematics

The ROM of the shoulder and elbow in the push and recovery phases at four different axle positions at the 'speed bump' cycle are shown in Table 7.

A specific trend of a significant difference in ROM of the shoulder in flexion/extension (in the sagittal plane), in internal/external rotation (in the transverse plane) and ROM of the elbow in flexion/extension (in the sagittal plane) was recognised in vertically adjusted axle positions such as upward and downward, but, there was no significant difference of ROM of all joints noted between horizontally adjusted axle positions such as forward and backward. The results from two-

Table 3. The post-hoc pairwise comparison for different axle positions in peak force total.

Pairwise comparisons						
Measure: peak force total						
					95% confidence interval for difference[a]	
(I) position	(J) position	Mean difference (I − J)	Std. error	*p*-Value[a]	Lower bound	Upper bound
UF	UB	−21.347	6.599	0.003**	−34.789	−7.905
	DF	−7.785	5.135	0.139	−18.245	2.675
	DB	−6.247	6.662	0.355	−19.817	7.324
UB	UF	21.347	6.599	0.003**	7.905	34.789
	DF	13.562	5.700	0.023*	1.951	25.172
	DB	15.100	8.321	0.079	−1.850	32.050
DF	UF	7.785	5.135	0.139	−2.675	18.245
	UB	−13.562	5.700	0.023*	−25.172	−1.951
	DB	1.538	5.194	0.769	−9.041	12.118
DB	UF	6.247	6.662	0.355	−7.324	19.817
	UB	−15.100	8.321	0.079	−32.050	1.850
	DF	−1.538	5.194	0.769	−12.118	9.041

[a]Adjustment for multiple comparisons: Least Significant Difference (equivalent to no adjustments).
*$p < 0.05$; **$p < 0.01$.

Table 4. Push rim variables at 'speed bump' push in upper and down positions.

				95% confidence interval		
Measure	Place	Mean	Std. error	Lower bound	Upper bound	*p*-Value
Peak total force (N)	Upper	112.27	4.78	102.71	121.82	0.655
	Down	109.23	4.78	99.67	118.78	
Peak moment M_z (Nm)	Upper	18.61	0.92	16.76	20.45	0.247
	Down	20.14	0.92	18.29	21.98	
Peak tangent force (N)	Upper	72.35	3.59	65.17	79.52	0.246
	Down	78.29	3.59	71.11	85.47	
Ave total force (N)	Upper	86.09	3.53	79.03	93.14	0.160
	Down	78.99	3.53	71.93	86.05	
Ave moment M_z (Nm)	Upper	12.34	0.52	11.29	13.39	0.531
	Down	12.81	0.52	11.76	13.85	
Ave. tangent force (N)	Upper	47.98	2.03	43.92	52.05	0.530
	Down	49.80	2.03	45.73	53.86	
Push angle (°)	Upper	64.55	3.52	57.52	71.58	0.773
	Down	65.99	3.52	58.96	73.02	
Ave speed (m/s)	Upper	0.90	0.03	0.84	0.95	0.950
	Down	0.89	0.03	0.84	0.95	
Mechanical effectiveness	Upper	0.57	0.02	0.53	0.61	0.025*
	Down	0.64	0.02	0.60	0.68	
Push frequency (1/s)	Upper	1.13	0.05	1.03	1.22	0.391
	Down	1.07	0.05	0.98	1.17	

*$p < 0.05$; **$p < 0.01$.

Table 5. Push rim variables at 'speed bump' push in forward and back positions.

				95% confidence interval		
Measure	Place	Mean	Std. error	Lower bound	Upper bound	*p*-Value
Peak total force (N)	Forward	103.07	4.03	95.02	111.12	0.008**
	Back	118.42	4.72	108.99	127.86	
Peak moment M_z (Nm)	Forward	17.92	0.67	16.58	19.25	0.003**
	Back	20.83	0.92	18.99	22.66	
Peak tangent force (N)	Forward	69.66	2.59	64.48	74.83	0.003**
	Back	80.98	3.57	73.84	88.12	
Ave. total force (N)	Forward	77.01	2.93	71.15	82.86	0.014**
	Back	88.07	3.68	80.72	95.43	
Ave. moment M_z (Nm)	Forward	11.88	0.37	11.15	12.62	0.017*
	Back	13.26	0.54	12.18	14.35	
Ave. tangent force (N)	Forward	46.21	1.43	43.35	49.08	0.017*
	Back	51.57	2.11	47.35	55.78	
Push angle (°)	Forward	63.20	3.20	56.81	69.58	0.386
	Back	67.34	3.67	60.01	74.68	
Ave. speed (m/s)	Forward	0.86	0.03	0.81	0.91	0.068
	Back	0.93	0.03	0.87	0.99	
Mechanical effectiveness	Forward	0.61	0.02	0.57	0.65	0.657
	Back	0.60	0.02	0.56	0.64	
Push frequency (1/s)	Forward	1.04	0.04	0.96	1.11	0.053
	Back	1.16	0.05	1.05	1.27	

*$p < 0.05$; **$p < 0.01$.

Table 6. Push rim variables at 'speed bump' push in four positions together.

Measure	Places	Mean	Std. error	95% confidence interval		*p*-Value
				Lower bound	Upper bound	
Peak total force (N)	Upper					
	Forward	95.17	5.70	83.79	106.55	0.001**
	Back	129.36	6.68	116.02	142.71	
	Down					
	Forward	110.97	5.70	99.59	122.35	
	Back	107.48	6.68	94.14	120.83	
Peak moment M_z (Nm)	Upper					
	Forward	16.34	0.94	14.46	18.23	0.088
	Back	20.87	1.30	18.28	23.47	
	Down					
	Forward	19.49	0.94	17.61	21.37	
	Back	20.78	1.30	18.19	23.38	
Peak tangent force (N)	Upper					
	Forward	63.54	3.66	56.23	70.86	0.088
	Back	81.15	5.05	71.06	91.25	
	Down					
	Forward	75.77	3.66	68.45	83.09	
	Back	80.81	5.05	70.72	90.90	
Ave total force (N)	Upper					
	Forward	72.51	4.14	64.24	80.79	0.001**
	Back	99.66	5.21	89.26	110.07	
	Down					
	Forward	81.50	4.14	73.23	89.78	
	Back	76.48	5.21	66.08	86.88	
Ave moment M_z (Nm)	Upper					
	Forward	11.10	0.52	10.06	12.15	0.055
	Back	13.57	0.77	12.04	15.11	
	Down					
	Forward	12.66	0.52	11.62	13.70	
	Back	12.95	0.77	11.42	14.48	
Ave tangent force (N)	Upper					
	Forward	43.18	2.03	39.13	47.23	0.055
	Back	52.78	2.98	46.82	58.74	
	Down					
	Forward	49.24	2.03	45.19	53.29	
	Back	50.35	2.98	44.39	56.31	
Push angle (°)	Upper					
	Forward	62.72	4.52	53.69	71.75	0.918
	Back	66.38	5.19	56.01	76.75	
	Down					
	Forward	63.67	4.52	54.64	72.70	
	Back	68.31	5.19	57.94	78.68	
Ave speed (m/s)	Upper					
	Forward	0.82	0.04	0.75	0.90	0.076
	Back	0.97	0.04	0.88	1.05	
	Down					
	Forward	0.89	0.04	0.82	0.96	
	Back	0.89	0.04	0.81	0.98	
Mechanical effectiveness	Upper					
	Forward	0.60	0.03	0.55	0.65	0.08
	Back	0.55	0.03	0.49	0.60	
	Down					
	Forward	0.62	0.03	0.57	0.67	
	Back	0.65	0.03	0.60	0.71	
Push frequency (1/s)	Upper					
	Forward	1.05	0.05	0.95	1.16	0.674
	Back	1.21	0.08	1.05	1.36	
	Down					
	Forward	1.02	0.05	0.92	1.13	
	Back	1.12	0.08	0.97	1.28	

*$p < 0.05$; **$p < 0.01$.

way ANOVA showed that there were no significant differences with combinate four positions. At 'the speed bump' cycle particularly in the push phase, ROM in abduction/adduction (in the frontal plane) followed a similar trend of significant difference in vertically adjusted axle positions. All the participants used an arching pattern of propulsion in which the hand followed an arc along the push rim in the recovery phase and was brought back in contact with the push rim for the next push. From Figure 7, it is clear that in the

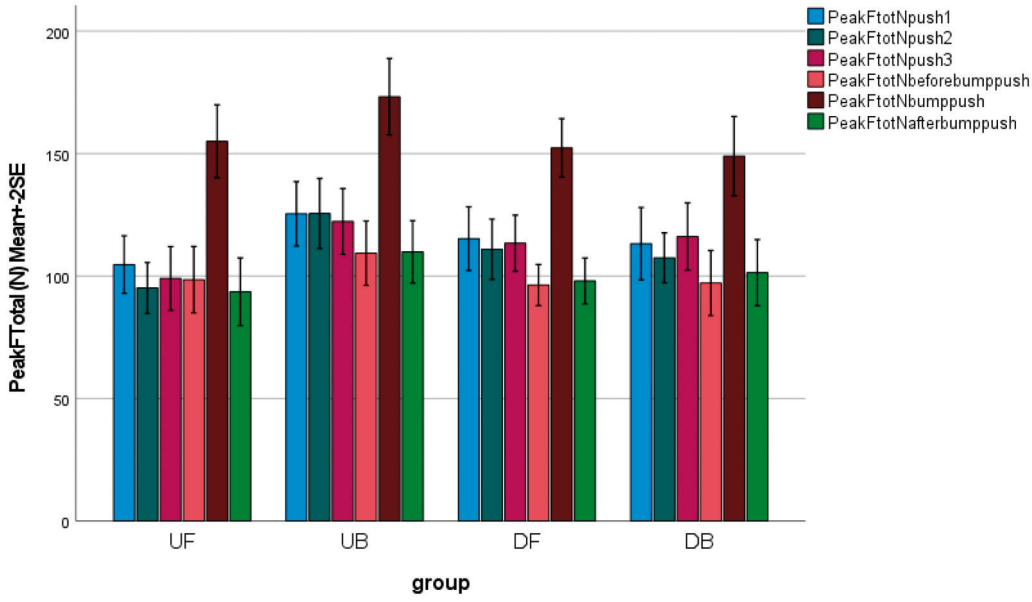

Figure 5. Peak total forces (N) at six pushes in four axle positions.

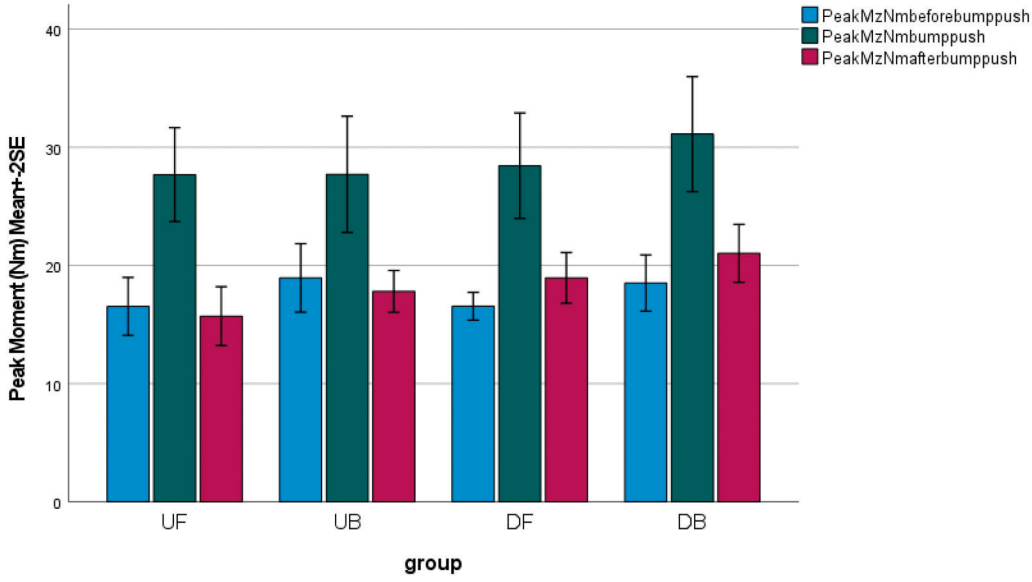

Figure 6. Peak moment (Nm) at 'before bump' push, at 'speed bump' push and at 'after speed bump'.

initial period of the push phase, the elbow joint (Graph A) was in maximum flexion. As the push phase progressed, extension constantly increased until the end of the push phase. Initiation of the recovery phase coincided with flexion of the elbow joint which constantly remained in flexion until the end of the recovery phase. At the start of the push phase, the shoulder (Graph B) was in maximum extension and progressed to flexion in the push phase. Although the arm remained abducted (Graph C) throughout the entire cycle, abduction decreased considerably in the push phase and the maximum decrease was seen at the 'speed bump' cycle followed by a constant increase in the recovery phase to reach the hand rim for the next push. A pattern of decreasing internal rotation (Graph D) during the push phase and increasing internal rotation during the recovery phase was recognised. The shoulder remained maximally extended and internally rotated at the beginning of the push phase and minimally abducted and internally rotated near the end of the push phase.

3.4. Subjective finding

After completion of data collection for each volunteer, all were asked about their choice for the most comfortable axle position out of the four tested. Out of 16

Table 7. Range of motion at the elbow and shoulder at speed bump push phase.

Measure	Mean	Std. error	95% confidence interval Lower bound	Upper bound	*p*-Value
ElbowFlexExtRoM					
Forward	42.6	1.2	40.3	44.9	0.430
Back	41.3	1.1	39.2	43.5	
ShoulderFlexExtRoM					
Forward	55.2	1.1	52.9	57.5	0.361
Back	53.8	1.1	51.6	55.9	
ShoulderAddAbuRoM					
Forward	12.6	0.4	11.7	13.4	0.953
Back	12.6	0.4	11.8	13.4	
ShoulderRotRoM					
Forward	43.1	1.3	40.5	45.8	0.966
Back	43.1	1.3	40.5	45.6	
ElbowFlexExtRoM					
Upper	46.3	1.0	44.3	48.3	<.0001**
Down	37.6	1.0	35.6	39.7	
ShoulderFlexExtRoM					
Upper	62.4	1.1	60.2	64.5	<.0001**
Down	46.6	0.8	44.9	48.2	
ShoulderAddAbuRoM					
Upper	13.4	0.4	12.5	14.2	0.004
Down	11.8	0.4	11.0	12.6	
ShoulderRotRoM					
Upper	52.5	1.4	49.8	55.2	<.0001**
Down	33.7	0.9	32.0	35.4	
ElbowFlexExtRoM					
Forward					
Upper	46.1	1.5	43.2	49.1	0.209
Down	39.1	1.5	36.1	42.0	
Back					
Upper	46.5	1.4	43.7	49.2	
Down	36.2	1.4	33.4	39.0	
ShoulderFlexExtRoM					
Forward					
Upper	63.3	1.6	60.2	66.4	0.67
Down	47.1	1.2	44.7	49.5	
Back					
Upper	61.4	1.5	58.4	64.4	
Down	46.1	1.1	43.9	48.4	
ShoulderAddAbuRoM					
Forward					
Upper	13.5	0.6	12.3	14.7	0.559
Down	11.6	0.6	10.5	12.7	
Back					
Upper	13.2	0.6	12.1	14.4	
Down	12.0	0.5	10.9	13.0	
ShoulderRotRoM					
Forward					
Upper	52.2	2.0	48.3	56.1	0.59
Down	34.1	1.3	31.6	36.6	
Back					
Upper	52.8	1.9	49.1	56.5	
Down	33.3	1.2	30.9	35.7	

*$p < 0.05$; **$p < 0.01$.

participants, 12 marked the UB axle position, three chose UF and one selected DF as the most comfortable axle position out of the four.

4. Discussion

This project collected kinematic and kinetic data from participants who propelled a wheelchair over a speed bump and tried to find which axle position would be optimum during propulsion in terms of biomechanical parameters.

4.1. Kinetics

The present study revealed that both peak total force and average total force were significantly higher in the UB axle position as compared to the other three axle positions at the speed bump position. Perhaps, the key point to note here is that the average speed was higher in the UB axle position as compared to the other three positions. Previously, some studies (Medola et al. 2014; Kotajarvi et al. 2004; Richter 2001) reported results on wheelchair pushing and axle position. Cowan et al. (2009) found no change in push angle and frequency in the horizontal adjustment of axle position. Kotajarvi et al. (2004) found no difference in push frequency and speed with change in axle positions during level propulsion. Kotajarvi et al. (2004) also found that there was no significant change in tangential force and there was no significant difference in fractional effective force (F_t/F_{tot}) which can be compared with mechanical efficiency with different axle positions. However, Kotajarvi et al. (2004) included paraplegics whereas the present study involved healthy novice non-wheelchair users. van der Woude et al. (1989) and Medola et al. (2014) also found that decreased push angle and increased frequency in the downward axle positions have a detrimental effect on fatigability and joint pathologies. Although Boninger et al. (2000) and Freixes et al. (2010) tested different axle positions, their set-ups were different from the present study, thus it is difficult to compare results. As we know, the current study is the first one to report a set of kinetic and kinematic parameters during wheelchaired propulsion at a speed bump.

A correlation between forces acting on the shoulder and symptomatic shoulder pain was investigated by Mercer et al. (2006). In the present study, the result of a rise in peak total force by approximately 50% at the 'speed bump' push as compared to 'before bump' push and 'after speed bump' push seems to be consistent with Nagy et al. (2012). To the best of our knowledge, no studies have previously documented peak moments in relation to obstacle negotiation thus, this parameter cannot be compared and here we recommend further investigation.

4.2. Kinematics

All participants used an arching pattern of propulsion which mirrors the observations of Qi et al. (2012). In most instances, the ROM of the shoulder and elbow

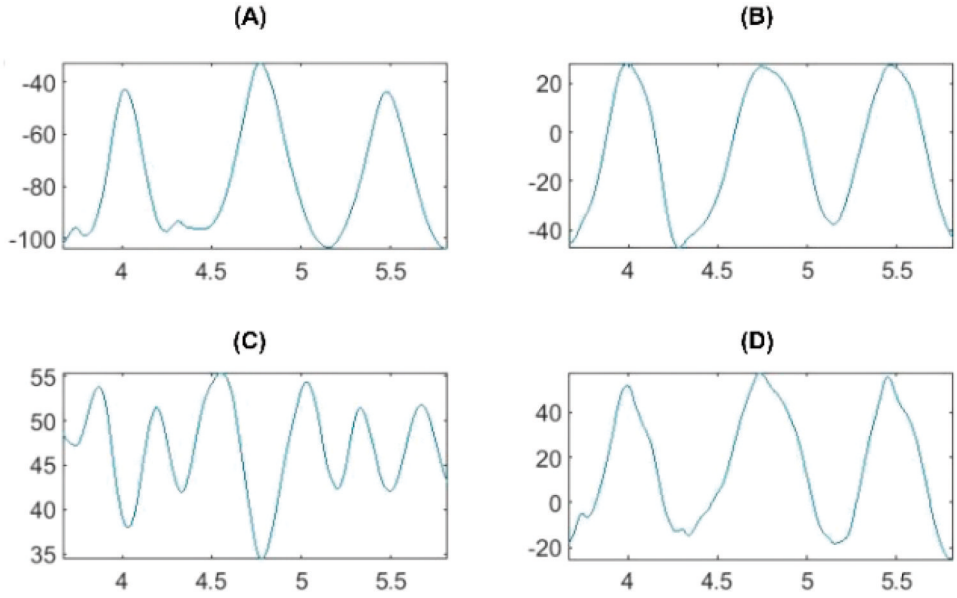

Figure 7. Graphical representation of Elbow and Shoulder motion during three cycles in a typical trial. Note: The horizontal axis is time with the unit as seconds, including three push cycles, that is, before bump, on bump and after bump push, and the vertical axis is the motion in different joints and planes. (A) Elbow flexion/extension in sagittal plane, (B) Shoulder flexion/extension in sagittal plane, (C) Shoulder abduction/adduction in frontal plane, (D) Shoulder internal/external rotation in transverse plane.

followed a specific trend of having a significant difference in vertically adjusted axle positions and no significant difference in horizontally adjusted axle positions. The most distinct and clinically important finding emerging from the present study analysis was that there was increased ROM of the shoulder and elbow in all the respective planes in the upward axle positions as compared to the downward axle positions. This trend seems to be consistent with previous research by Kotajarvi et al. (2004) and Medola et al. (2014). In contrast, Freixes et al. (2010) observed decreased internal rotation in the UF axle position and no significant difference in sagittal and frontal plane ROM.

Meanwhile, Hassanain et al. (2018) found increased ROM in the posterior axle position as compared to the anterior position. Moreover, they observed ROM of the shoulder in flexion/extension (40.02°±12.35°), in abduction/adduction (24.63°±6.38°) and in internal/external rotation (17.31°±4.27°) which differs from results of the present study. A probable explanation is that they used 3 cm and 6 cm backward positions from the manufacturer's position which shows variation in methodology and varies the results.

4.3. Limitations

The main challenge faced during this project was an improper blue tooth connection between the Smartwheel® and its workstation. Moreover, it stopped connecting during the project and as a result, the data collection was stopped which resulted in a sample size of 16 only. Despite the novel observations of this present project, it is not without limitations. This project was performed in a sports laboratory on a hard, smooth vinyl floor due to the non-portability of various equipment whereas, in day-to-day life, users must propel a wheelchair on concrete roads, grass, carpet, all of which have different rolling resistance. Variability in speed may have introduced another confounding factor for analysis. We recommend recording anthropometric measurements of the upper limb of each individual which would give moments at particular joints. In the present study, only extreme adjustments were evaluated however, we suggest that other axle positions should also be considered in future research.

4.4. Sweet spot

There have been some previous studies on whether the axle position of a wheelchair could correlate with biomechanical parameters and electromyography (EMG), but there is a lack of confirmed conclusion (Boninger et al. 2005). Objectively, this study reports that the UF position tends to contribute to larger contact angle, reduced stroke frequency, and diminished rate of rising of peak force. UF also positions the rear wheel in a more comfortable position relative to the user such that it is easier to use a large contact angle without having to strain to reach the top dead centre

of the handrim. In essence, the wheel is directly under the user rather than behind them. Therefore, UF could be suggested to be the sweet spot in clinical practice. Subjectively, novice users who were in this study may prefer the UB because it makes a chair more stable, however, adds rolling resistance to the system because the casters are loaded and the centre of mass is shifted forward. Theoretically, it is still not clear why the UF axle position reduces the push forces. This topic should be investigated further in the future, maybe using an inverse dynamic model to estimate muscle forces in the upper limbs.

5. Conclusion

This study provides the first comprehensive assessment of kinetics, upper limb kinematics and movements of the shoulder in able-bodied subjects during wheelchair propulsion while negotiating a standard speed bump of 6 cm height. It has been concluded that with the UF axle position, propulsion ergonomics is significantly best-concerning peak force. However, ROM is increased in the UF position but, is still within the normal range. If instability is an issue during axle position adjustment, then the axle can be moved backwards gradually until stability is achieved. This knowledge may help when prescribing, designing and selecting wheelchairs to provide the proper comfort and functionality for the user thus, promoting users' social participation, independence and better quality of life.

This study suggests the increased push rim forces with a 50% rise in peak force and approximately 60–80% rise in peak moment to negotiate a speed bump of 6 cm height. The peak total force at the 'speed bump' push was even greater than that of the first three pushes by 30%. This will also help to evaluate progress during different rehabilitation programmes such as muscle strengthening or during training of new wheelchair users, meaning adequate rehabilitation is required before considering additional skills of negotiation of obstacles. From the findings, it is suggested that the manufactures of gloves could enhance the materials to protect hands, and clinically in rehabilitation, patients with shoulder injury should avoid going over bumps, as the pushing forces are 50% greater when the wheelchair crosses over the bump than those on level ground.

Authors' contributions

MG: data collection, data analysis and writing of the paper; PW, GA, SN, RA: data collection and analysis; WW: design of the project, data analysis, modelling and writing of the paper.

Acknowledgements

The authors would like to thank Dr Tim Drew, Mr Ian Christie, Mr Gordon Spark and the wheelchair department at the TORT Centre for their support during the study.

Disclosure statement

No potential conflict of interest was reported by the author(s).

Funding

The author(s) reported there is no funding associated with the work featured in this article.

ORCID

Peng Wang http://orcid.org/0000-0003-3987-9270

References

Boninger, M., M. Baldwin, R. Cooper, A. Koontz, and L. Chan. 2000. "Manual Wheelchair Push Rim Biomechanics and Axle Position." *Archives of Physical Medicine and Rehabilitation* 81 (5): 608–613. doi:10.1016/S0003-9993(00)90043-1.

Boninger, M., R. Waters, T. Chase, M. Dijkers, H. Gellman, R. Gironda, B. Goldstein, S. Johnson-Taylor, A. Koontz, and S. McDowell. 2005. "Preservation of Upper Limb Function following Spinal Cord Injury, a Clinical Practice Guideline for Health-Care Professionals." *J Spinal Cord Med* 28: 434–470.

Briley, S. J., R. J. K. Vegter, V. L. Tolfrey, and B. S. Mason. 2020. "Propulsion Biomechanics Do Not Differ between Athletic and Nonathletic Manual Wheelchair Users in Their Daily Wheelchairs." *Journal of Biomechanics* 104: 109725. doi:10.1016/j.jbiomech.2020.109725.

Cowan, R., M. Nash, J. Collinger, A. Koontz, and M. Boninger. 2009. "Impact of Surface Type, Wheelchair Weight, and Axle Position on Wheelchair Propulsion by Novice Older Adults." *Archives of Physical Medicine and Rehabilitation* 90 (7): 1076–1083. doi:10.1016/j.apmr.2008.10.034.

Desroches, G., D. Pradon, C. Bankolé, R. Dumas, and L. Chèze. 2009. "Upper Limb Joint Moments during Wheelchair Obstacle Climbing." *Computer Methods in Biomechanics and Biomedical Engineering* 12 (sup1): 99–100. doi:10.1080/10255840903077311.

Dubowsky, S., S. Sisto, and N. Langrana. 2009. "Comparison of Kinematics, Kinetics, and EMG throughout Wheelchair Propulsion in Able-Bodied and Persons with Paraplegia: An Integrative Approach." *Journal of Biomechanical Engineering* 131 (2): 021015. doi:10.1115/1.2900726.

Freixes, O., S. Fernández, M. Gatti, M. Crespo, L. Olmos, and I. Rubel. 2010. "Wheelchair Axle Position Effect on Start-up Propulsion Performance of Persons with Tetraplegia."

Journal of Rehabilitation Research and Development 47 (7): 661–668.

Hassanain, A., R. Guppy, G. Whatling, and C. Holt. 2018. "Impact of Rear Wheel Axle Position on Upper Limb Kinematics and Electromyography during Manual Wheelchair Use." *International Biomechanics* 5 (1): 17–29. doi:10.1080/23335432.2018.1457983.

Kabra, C., R. Jaiswal, G. Arnold, R. Abboud, and W. Wang. 2015. "Analysis of Hand Pressures Related to Wheelchair Rim Sizes and Upper-Limb Movement." *International Journal of Industrial Ergonomics* 47: 45–52. doi:10.1016/j.ergon.2015.01.015.

Koontz, A. M., R. A. Cooper, M. L. Boninger, Y. Yang, B. G. Impink, and L. H. V. van der Woude. 2005. "A Kinetic Analysis of Manual Wheelchair Propulsion during Start-up on Select Indoor and Outdoor Surfaces." *The Journal of Rehabilitation Research and Development* 42 (4): 447–458. doi:10.1682/JRRD.2004.08.0106.

Kolwadkar, Y., S. Brown, R. Abboud, and W. Wang. 2011. "Comparison of Two Actuation Systems for Laparoscopic Surgical Manipulators Using Motion Analysis." *Surgical Endoscopy* 25 (3): 964–974. doi:10.1007/s00464-010-1300-y.

Kotajarvi, B., M. Sabick, K. An, K. Zhao, K. Kaufman, and J. Basford. 2004. "The Effect of Seat Position on Wheelchair Propulsion Biomechanics." *The Journal of Rehabilitation Research and Development* 41 (3b): 403–414. doi:10.1682/JRRD.2003.01.0008.

Louis, N., and P. Gorce. 2010. "Surface Electromyography Activity of Upper Limb Muscle during Wheelchair Propulsion: Influence of Wheelchair Configuration." *Clinical Biomechanics (Bristol, Avon)* 25 (9): 879–885. doi:10.1016/j.clinbiomech.2010.07.002.

MacGillivray, M. K., J. J. Eng, E. Dean, and B. J. Sawatzky. 2020. "Effects of Motor Skill-Based Training on Wheelchair Propulsion Biomechanics in Older Adults: A Randomized Controlled Trial." *Archives of Physical Medicine and Rehabilitation* 101 (1): 1–10. doi:10.1016/j.apmr.2019.07.017.

Medola, F., V. Elui, C. da Santana, and C. Fortulan. 2014. "Aspects of Manual Wheelchair Configuration Affecting Mobility: A Review." *Journal of Physical Therapy Science* 26 (2): 313–318. doi:10.1589/jpts.26.313.

Mercer, J., M. Boninger, A. Koontz, D. Ren, T. Dyson-Hudson, and R. Cooper. 2006. "Shoulder Joint Kinetics and Pathology in Manual Wheelchair Users." *Clinical Biomechanics (Bristol, Avon)* 21 (8): 781–789. doi:10.1016/j.clinbiomech.2006.04.010.

Nagy, J., A. Winslow, J. M. Brown, L. Adams, K. O'Brien, M. Boninger, and G. Nemunaitis. 2012. "Pushrim Kinetics during Advanced Wheelchair Skills in Manual Wheelchair Users with Spinal Cord Injury." *Topics in Spinal Cord Injury Rehabilitation* 18 (2): 140–142. doi:10.1310/sci1802-140.

Paralyzed Veterans of America. 2005. *Preservation of Upper Limb Function following Spinal Cord Injury: A Clinical Practice Guideline for Health-Care Professionals*. Washington, DC: Paralyzed Veterans of America.

Qi, L., J. Wakeling, S. Grange, and M. Ferguson-Pell. 2012. "Effect of Velocity on Shoulder Muscle Recruitment Patterns during Wheelchair Propulsion in Nondisabled Individuals: Pilot Study." *The Journal of Rehabilitation Research and Development* 49 (10): 1527–1536. doi:10.1682/JRRD.2011.03.0047.

Quickie GPV Range, Owner's manual, Sunrise® Medical Limited, West Midlands, England. Page no.33.

Richter, W. 2001. "The Effect of Seat Position on Manual Wheelchair Propulsion Biomechanics: A Quasi-Static Model-Based Approach." *Medical Engineering & Physics* 23 (10): 707–712. doi:10.1016/s1350-4533(01)00074-1.

Robertson, R., M. Boninger, R. Cooper, and S. Shimada. 1996. "Push Rim Forces and Joint Kinetics during Wheelchair Propulsion." *Archives of Physical Medicine and Rehabilitation* 77 (9): 856–864. doi:10.1016/S0003-9993(96)90270-1.

Sherif, S., S. Hasan, G. Arnold, R. Abboud, and W. Wang. 2016. "Analysis of Hand Pressure in Different Crutch Lengths and Upper-Limb Movements during Crutched Walking." *International Journal of Industrial Ergonomics* 53C: 59–66. doi:10.1016/j.ergon.2015.10.010.

Silva, D. C., L. C. Paschoarelli, and F. O. Medola. 2019. "Evaluation of Two Wheelchair Hand Rim Models: Contact Pressure Distribution in Straight Line and Curve Trajectories." *Ergonomics* 62 (12): 1563–1571. doi:10.1080/00140139.2019.1660000.

Stone, B., B. S. Mason, A. Bundon, and V. L. Goosey-Tolfrey. 2019. "Elite Handcycling: A Qualitative Analysis of Recumbent Handbike Configuration for Optimal Sports Performance." *Ergonomics* 62 (3): 449–458. doi:10.1080/00140139.2018.1531149.

Three Rivers Holdings. 2008. *Smartwheel® User's Guide*. Mesa, AZ: Three Rivers Holdings, LLC.

van der Woude, L., D. Veeger, R. Rozendal, and T. Sargeant. 1989. "Seat Height in Hand Rim Wheelchair Propulsion." *Journal of Rehabilitation Research and Development* 26: 31–50.

Weston, E. B., S. N. Khan, and W. S. Marras. 2017. "Wheelchair Pushing and Turning: Lumbar Spine and Shoulder Loads and Recommended Limits." *Ergonomics* 60 (12): 1754–1765. doi:10.1080/00140139.2017.1344445.

Wieczorek, B., and M. Kukla. 2019. "Effects of the Performance Parameters of a Wheelchair on the Changes in the Position of the Centre of Gravity of the Human Body in Dynamic Condition." *PLoS One* 14 (12): e0226013. doi:10.1371/journal.pone.0226013.

Wu, G., F. C. T. van der Helm, H. E. J. D. Veeger, M. Makhsous, P. Van Roy, C. Anglin, J. Nagels, A. R. Karduna, K. McQuade, X. Wang, F. W. Werner, and B. Buchholz. 2005. "ISB Recommendation on Definitions of Joint Coordinate Systems of Various Joints for the Reporting of Human Joint Motion—Part II: Shoulder, Elbow, Wrist and Hand." *Journal of Biomechanics* 38 (5): 981–992.